Iron(III) and Zinc(II) Metal Alkaloid Complexes: Synthesis, Characterization and Biological Activities

Bushra Naureen[1*], G. A. Miana[2], Khadija Shahid[2], Mehmood Asghar[3,4], Samreen Tanveer[5], Muhammad Faheem[2], Aziza Sarwar[1,6], Ahmad Danial Azzahari[7]

[1]Department of Chemistry, Faculty of Science, Universiti Malaya, 50603 Kuala Lumpur, Malaysia
[2]Riphah Institute of Pharmaceutical Sciences, Riphah International University, 44000 Islamabad, Pakistan
[3]Department of Restorative Dentistry, Faculty of Dentistry, Universiti Malaya, 50603 Kuala Lumpur, Malaysia
[4]Department of Biological Sciences, National University of Medical Sciences, The Mall, Abid Majeed Road, Rawalpindi, Punjab 46000, Pakistan
[5]Faculty of Pharmacy, University of Central Punjab, Khayaban-e-Jinnah Road, Johar Town, Lahore, Pakistan
[6]Department of Chemistry, Faculty of Science, Balochistan University of Information Technology, Engineering and Management Sciences, Quetta, Pakistan
[7]Centre for Foundation Studies in Science, Universiti Malaya, 50603 Kuala Lumpur, Malaysia
*Corresponding author (e-mail: bushranauren@gmail.com)

Alkaloids possess various pharmacological actions and hence are considered as active biological moieties. Metal ions are essential for the normal functioning of the human body and any deficiency may cause diseases. In biomedical sciences, alkaloid metal ion complex formation has become a significant research area. In this study, three alkaloid ligands (L1, L2 and L3) underwent metal complex formation to produce iron(III) and zinc(II) metal complexes. Later, the biological activities of these alkaloid ligands and their iron(III) and zinc(II) metal complexes were investigated. These ligands and their metal complexes were characterized using ultraviolet-visible spectroscopy (UV-Vis), fourier-transform infrared spectroscopy (FTIR), nuclear magnetic resonance spectroscopy (NMR) and mass spectrometry (MS). Pharmacological tests including antibacterial, antifungal, antioxidant and antitumor assays were performed. All compounds showed antibacterial and antifungal activity, but the metal complexes showed better activities than the original ligands, especially the zinc(II) complexes of all ligands. All compounds showed more significant antifungal activity against *Candida albicans* than *Candida glabrata*. Free ligands illustrated better antioxidant behaviour and antitumour activity compared to the metal complexes. Thus, both ligands and their metal complexes, being active agents, should be explored further particularly with reference to their mechanism of action

Key words: Alkaloid; metal complex; antibacterial; antifungal; antioxidant; antitumour

Received: November 2020; Accepted: March 2021

The term "alkaloid" (meaning alkali-like) was first assigned to all organic bases isolated from plants. Hence these alkaloids were also termed as plant alkaloids or vegetable alkaloids. Now alkaloids are more appropriately defined as nitrogen-containing moieties with low molecular weights occurring mainly in plants, but also to some extent in animals and microorganisms. Nitrogen atoms present in alkaloids can be one or more in number, and these confer basicity to the alkaloids, but the degree of basicity greatly varies depending on the alkaloid structure and the location of the functional groups present. However, some alkaloids may be neutral as well, where nitrogen acts as part of the amide function [1, 2]. Generally, tyrosine and tryptophan alkaloidal derivatives are classified biosynthetically as isoquinoline and quinoline alkaloids, respectively. Quinoline and isoquinoline were first isolated from coal tar in 1834 and 1835, respectively**.**

Quinoline is employed as a solvent in organic synthesis. The boiling point of quinoline is high, whereas the melting point of isoquinoline is low. The basicity values of both quinoline (pK_a=4.9) and isoquinoline (pK_a=5.1) are moderate. Both compounds are mostly derived from flowering plants; however, animals and microorganisms can be good sources [3].

Tetrahydroisoquinolines (TIQs) have been reported to be potent biological agents. A key intermediate common to most biosynthetic pathways is

the tetrahydroisoquinoline heterocyclic nucleus. One of the TIQs which has been reported to possess extraordinary biological activity is (S)-3-aminoethyl-1,2,3,4-tetrahydroisoquinoline [4]. L-tyrosine, which is the main source of the derivation of benzylisoquinoline alkaloids (BIAs) which leads to the production of approximately 2500 specialized structures. The three main steps of BIA biosynthesis are benzylisoquinoline backbone formation (step 1), followed by benzylisoquinoline skeleton rearrangement (step 2), and addition of functional groups (step 3). BIAs include many important pharmaceuticals and semisynthetic drug precursors. Significant examples include morphine, codeine, sanguinarine, tubocurarine and papaverine [5].

Papaverine (melting point 147°C) is one of the most important benzylisoquinoline alkaloids. Opium (papaver somniferum) is the principal natural source of papaverine, along with morphine and other associated alkaloids. Papaverine was first isolated in 1848 from morphine mother liquor, and it was the first opium alkaloid whose structure was fully elucidated [6].

A variety of drugs with diverse pharmacological applications have quinoline and isoquinoline as a basic pillar of their structure. Argemonine possesses antitumor activity while the herpes simplex virus exhibits inhibitor activity. Berberine, sanguinarine and cinchonine all exhibit excellent antibacterial, antimalarial, antidiarrheal and antiprotozoal properties. Several studies have confirmed the analgesic and antitussive activities of morphine and codeine. Stepholidine acts as a dopamine D1 receptor agonist and a dopamine D2 receptor antagonist. All these alkaloids contain the quinoline and isoquinoline nucleus. [3, 7-16].

The importance of metal complexes of alkaloids has been acknowledged in the fields of bioinorganic chemistry, medicinal chemistry and drug design, owing to the ability of metals to form coordination complexes with a variety of other molecules [17]. Various metals are used to form complexes with alkaloids. Amongst them, iron(III) and zinc(II) are the most frequently used metals because of their associated biological properties such as antimicrobial activity [18-21]. Iron is hydrolyzed by acidic solutions, and its oxychloride is produced by heating to 350°C. Due to its strong Lewis acid nature, reaction with Lewis bases is common. Reaction with alkali metals leads to the production of metal alkoxide complexes. Both reducing and oxidizing properties are present in iron(III) chloride [22-24]. Being a leaching agent, it is used in chloride hydrometallurgy, e.g. Si production from FeSi in the Silgrain process [25]. The colorimetric method is used for phenol testing in which the radical reagent is ferric chloride [26]. Drinking water and sewage system purification processes require iron(III) chloride, which captures hydroxide ions, and forms iron(III) hydroxide flock [27].

Zinc(II) generally occurs both in anhydrous and hydrated forms, and is used in chemical synthesis and dietary preparations. The acetate group, by utilizing its two oxygen atoms (O_2), forms a linkage with metal ions, and its hydrate group also shows similar connections. A tetrahedral environment is produced by anhydrous zinc acetate, where zinc coordination occurs with four oxygen atoms. In contrast, an octahedral environment exists in the case of zinc acetate dihydrate. Acetic anhydride is lost if zinc acetate is heated in a vacuum, thus leaving a basic zinc acetate residue [28, 29]. Zinc deficiencies are treated by zinc acetate supplements. In the human body, copper absorption is inhibited by zinc acetate for the treatment of Wilson's disease. Ointments and topical lotions incorporate zinc acetate along with erythromycin for acne treatment. For treatment of the common cold, zinc lozenges are employed [30].

The current study is focused on introducing new antimicrobial agents, antioxidants and antitumor/anticancer drugs to overcome the issue of drug resistance and to minimize problems associated with side effects of existing drugs. For this purpose, alkaloids (Ligands 1, 2 and 3) were used, and their iron(III) and zinc(II) metal complexes were synthesized. Ligands and their metal complexes were characterized by spectral characterization techniques, including ultraviolet-visible spectroscopy (UV-Vis), fourier-transform infrared spectroscopy (FTIR), nuclear magnetic resonance spectroscopy (NMR) and mass spectrometry (MS). Pharmacological analyses such as antifungal, antibacterial, antioxidant and cytotoxicity assays were also performed.

MATERIALS AND METHODS

1. Chemicals

To perform biological activities and to synthesize metal complexes, high standard chemicals, as well as solvents, were employed and standard procedure [31, 32] was used for drying purposes, where needed. Acetone, benzene, ether, n-hexane and nutrient agar medium were purchased from Merck. Ascorbic acid, chloroform, dimethyl sulfoxide, sabouraud dextrose agar, sodium chloride and sodium hydroxide were obtained from Sigma Aldrich. Zinc acetate dihydrate and potassium hydroxide were supplied by BHD Chemicals. Methanol and ethanol were purchased from Fischer Chemicals, whereas ferric chloride anhydrous was obtained from RHD Chemicals.

2. Instrumentation

Ultraviolet-visible (UV-Vis) spectra were recorded on a UV-Vis spectrophotometer (Jasco Corporation Japan). Fourier transform infrared spectroscopy (FT-IR) spectra were collected on a Shimadzu FTIR spectrophotometer (Prestige-21), with attenuated total reflectance (ATR) 8000A accessory and a Bruker spectrometer (ATR, eco ZnSe, Vmax cm^{-1}), where the methodology for spectra recording was total reflectance. At room temperature, ^{13}C-NMR and ^{1}H-NMR spectra were plotted on a Bruker Avance NMR spectrophotometer AV 500 and ARX 300 MHz spectrometer. Dimethyl sulfoxide (DMSO-d6), spectroscopy grade, was used as a solvent for NMR analysis, and the internal standard was tetramethylsilane (TMS). High-resolution mass spectrometry was used to acquire mass spectra. Glassware from Wertlab (Germany) and Pyrex/Iwiki (Japan) were used. Analytical balance (Shimadzu, Japan), melting point apparatus (Gallenkamp U.S.A), hot plate magnetic stirrer (Velp), incubator (Memmert, Germany) and vortex of IR MECO were used. For volume reduction purposes, a complete rotary evaporator and aspirator system was employed (Eyela, Japan). For different biological activities, an autoclave (Hirayama, Japan) was used for sterilization.

3. Synthesis of Ligands

All alkaloid ligands (L1, L2 and L3) were gifted to us by Prof. Dr Maurice Shamma of Pennsylvania State University, USA [33]. The iron(III) and zinc(II) metal complexes of ligands (L1, L2 and L3) were synthesized in our labs by methods already reported in the literature [34]. The structures of the ligands (L1, L2 and L3) are shown in Figures 1, 2 and 3, respectively.

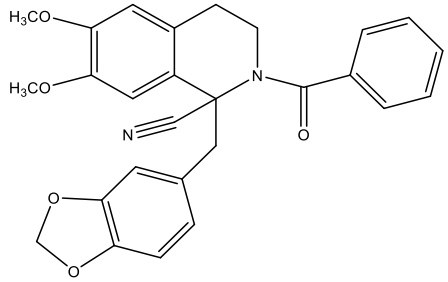

Figure 1. Structure of Ligand 1

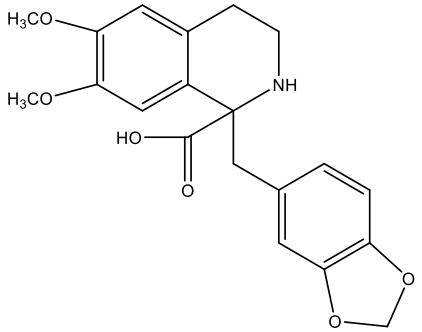

Figure 2. Structure of Ligand 2

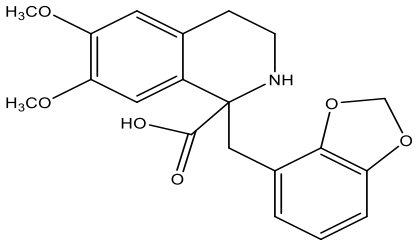

Figure 3. Structure of Ligand 3

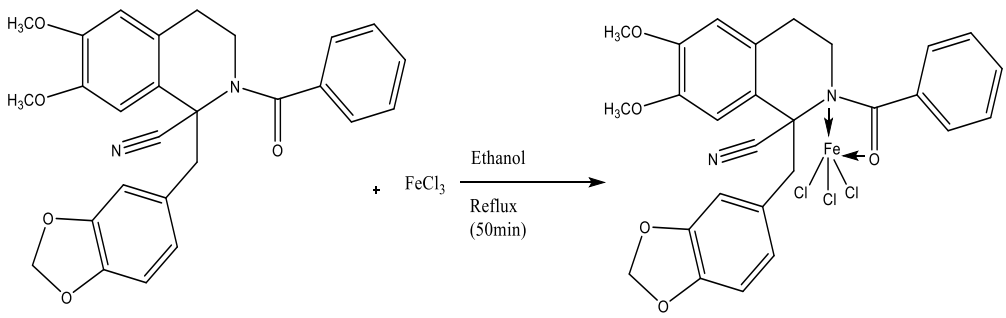

Figure 4. Synthesis of iron(III) complex of Ligand 1

4. Synthesis of Metal Complexes

4.1. Synthesis of Iron(III) Complexes of Ligands 1- 3

Solutions of ligand (1 mmol) and ferric trichloride (1 mmol) in 25 mL ethanol were prepared separately. Both solutions were mixed by magnetic stirring in round bottom flasks (250 mL). The resulting mixtures was refluxed for 50 minutes, at 78.5ºC with continuous stirring and cooled at room temperature. Filtration was conducted for the solid particles. Methanol was used for recrystallization and finally the solids were dried under vacuum. The synthesis of iron(III) complexes of Ligands 1-3 are represented in Figures 4, 5 and 6, respectively.

A brown coloured product of the iron(III) complex of Ligand 1 with a melting point 327ºC was collected. It was freely soluble in DMSO and ethanol, sparingly soluble in acetone, benzene, hexane, methanol, 1% NaOH and 0.9% NaCl and insoluble in chloroform and ether.

The iron(III) complex of ligand 2 was dark brown and its melting point was > 400ºC. It was freely soluble in DMSO and methanol, sparingly soluble in acetone, benzene, ethanol, ether, 1% NaOH and 0.9% NaCl and insoluble in chloroform and hexane.

The iron(III) complex of ligand 3 was maroonish brown in colour, with a melting point > 400ºC. The iron(III) complex was freely soluble in DMSO and ethanol, sparingly soluble in acetone, benzene, hexane, methanol, 1% NaOH and 0.9% NaCl and insoluble in chloroform and ether.

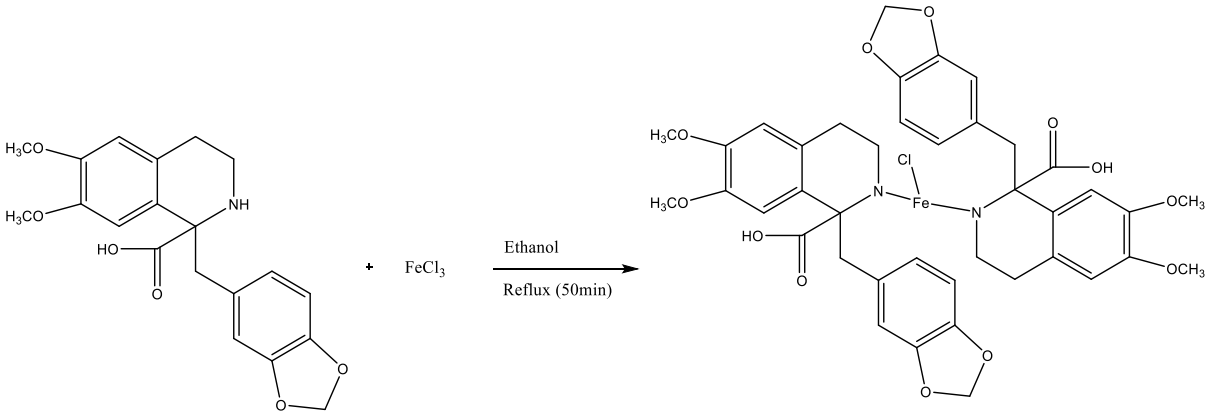

Figure 5. Synthesis of iron(III) complex of Ligand 2

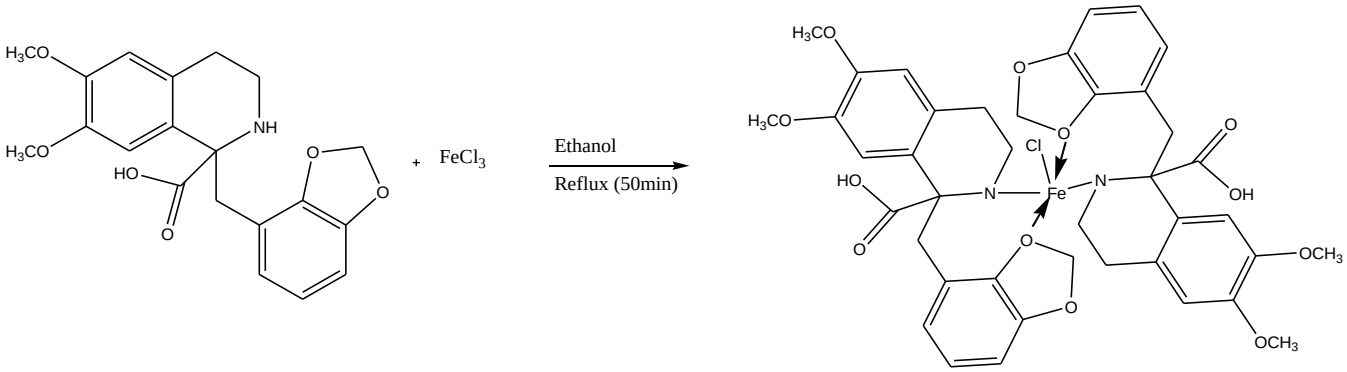

Figure 6. Synthesis of iron(III) complex of Ligand 3

4.2. Synthetic Schemes of Zinc(II) Complexes of Ligands 1-3

Zinc(II) complexes of Ligands 1-3 were prepared using the reported method [34]. Zinc acetate dihydrate (1 mmol) was dissolved in methanol (25 mL), and Ligand (1 mmol) was dissolved in methanol (25 mL) separately. After mixing, the pH of of the combined solution was adjusted (7.5 ± 0.5) using KOH solution (0.1% in methanol). The mixture was refluxed for 3 hours, at 65ºC, followed by removal of the solvent using a rotary evaporator. Methanol was used for washing the product, which was then dried. The synthesis of zinc(II) complexes of Ligands 1-3 are presented in Figures 7, 8 and 9, respectively.

A pale yellow product with a melting point of 272ºC was collected. It was freely soluble in DMSO, sparingly soluble in chloroform, ethanol, ether, methanol, 1% NaOH and 0.9% NaCl and insoluble in acetone, benzene and hexane.

A product with a skin brown colour and melting point 280ºC was obtained. This zinc(II) complex was freely soluble in DMSO, ethanol, ether and methanol, sparingly soluble in 1% NaOH and 0.9% NaCl and insoluble in acetone, benzene, chloroform and hexane.

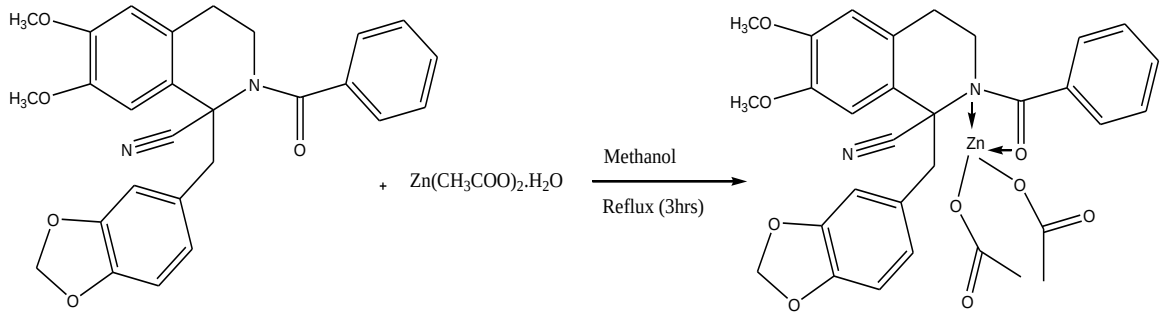

Figure 7. Synthesis of zinc(II) complex of Ligand 1

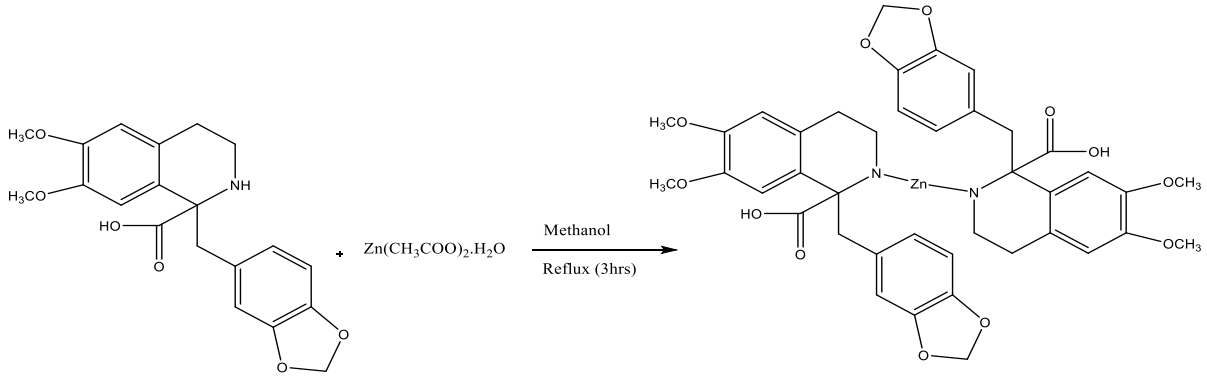

Figure 8. Synthesis of zinc(II) complex of Ligand 2

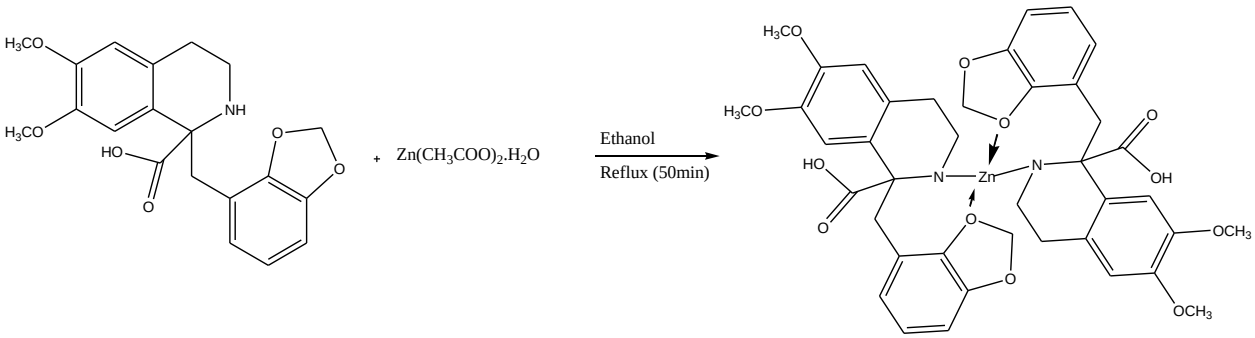

Figure 9. Synthesis of zinc(II) complex of Ligand 3

A clay-pink product with a melting point of 268ºC was obtained. This product was freely soluble in DMSO, ethanol, ether, methanol, 1% NaOH and 0.9 % NaCl and insoluble in acetone, benzene, chloroform and hexane.

The expected geometries of iron(III) complexes ($L1FeCl_3$, $(L2)_2FeCl$, $(L3)_2FeCl$) are trigonal bipyramidal, trigonal planar and square pyramidal. The expected geometries of zinc(II) complexes ($L1Zn(Ac)_2$, $(L3)_2Zn$) are square planar and $(L2)_2Zn$ is linear. Similar iron(III) and zinc(II) metal complex geometries have been reported in the literature [35-38].

5. Biological Screening/Evaluation

5.1. Antibacterial Activity Evaluation

Antibacterial screening was conducted in vitro, for all the ligands and their metal complexes against different bacterial strains, i.e. gram-positive (*Pseudomonas aeruginosa*) and gram-negative (*Escherichia coli*, *staphylococcus aureus*) by the agar well diffusion method [39]. The test organism, i.e. bacteria were inocculated in a nutrient broth (10 mL aliquot), and incubated at 37ºC ± 1ºC for 24 hours. The broth culture (0.6 mL) containing the test organism was incorporated inside cooled (45ºC) molten agar, which was adequately mixed and poured into sterile petri dishes. Duplicate plates were prepared for each organism. After solidification of the agar, a cork borer (sterile) was used for digging wells of 6 mm each, and the agar plugs were removed.

Individual solutions with a concentration of 1mg/mL were prepared for all the ligands and their metal complexes. A micropipette was used for transferring samples (100 µL approximately) into the wells which were labelled accurately. The positive control used was tetracycline (30 µg disc), and the negative control was methanol. For 2 hours, the petri plates were kept at room temperature for better sample diffusion. The petri plates faced upwards at 37ºC ± 1ºC temperature for incubation purposes, for 24 hours. The zone of inhibition for the determination of antibacterial activity was measured in millimetres (mm).

5.2. Antifungal Activity Evaluation

The two fungal strains used for antifungal evaluation of the test compounds were *Candida albicans* (*C.albicans*) and *Candida glabrata* (*C.glabrata*). After inoculating the fungi in sabouraud dextrose broth (SDB), 24 hours incubation was done at 28ºC, followed by matching the test organism concentration with 0.5 McFarland standard [40]. The well-in-agar method was employed for antifungal screening. A sterile cotton swab was used for loading the fungal culture, and the swab was firmly pressed against the tube's inside wall, for removal of the inoculum. For uniform distribution of the fungal cultures on the entire sabouraud dextrose agar medium (sterile), streaking with the swab was done thrice (the plate was rotated approximately 60° each time).

A cork borer (sterile) was used for boring holes of 6 mm diameter in the inoculated medium. Each hole was labelled appropriately and then filled with 50 µL of the test sample (1mg/mL) [41]. The standard drug used was nystatin, and methanol was the negative control. At room temperature, the plates were left for an hour, for better penetration of the standard drug and the test samples. After sealing the agar plates with Parafilm, they were incubated at 28ºC for 48 hours. Antifungal activity was indicated by the appearance of inhibition zones around the holes. These experiments were conducted in duplicate [42].

5.3. Antioxidant Activity Evaluation

The antioxidant activity of the test compounds was evaluated by employing a DPPH (2, 2-diphenyl-2-picrylhydrazyl hydrate) assay. DPPH is a stable free radical, against which the test compounds have spectrophotometrically shown radical scavenging activity. DPPH reduction occurred by attack of the hydrogen donating antioxidant moiety, which bleached its dark purple colour to yellow in methanol [43].

Final concentrations (500 µg/mL, 100 µg/mL, 50 µg/mL, 10 µg/mL and 5 µg/mL) were diluted from a stock solution of 1mg/mL. Sample solutions (3 mL) dissolved in 5% DMSO were added to 1 mL of methanolic DPPH solution (0.3mM). After vigorous shaking, the mixture was left in the dark for 30 minutes at room temperature. Then a UV-VIS spectrophotometer was used for measuring the absorbance at 517 nm. Greater free-radical scavenging activity was indicated if the absorbance showed by the mixture was reduced. Ascorbic acid was used as the standard, and the solvent was methanol. The following equation was used for the calculation of the radical scavenger effect of DPPH:

$$\text{scavenging effect}(\%)\frac{\text{Absorbance of control} - \text{Absorbance of sample}}{\text{Absorbance of control}} \times 100$$

Determination of IC_{50} (sample concentration required

for 50% DPPH radical scavenging) values was done by using GraphPad Prism software Version 6.01 [44].

5.4. Cytotoxicity Assays

5.4.1. Brine-shrimp Microwell Cytotoxicity Assay

Simulated seawater was prepared by dissolving sea salt (38 gm, NaCl non-ionized) in a litre of distilled (sterile) water, and a clear solution was obtained by filtration. The pH was maintained in the range of 8-9 using sodium bicarbonate ($NaHCO_3$) solution. A pet shop was the source of the test organism, Leach, i.e. Artemia salina (brine shrimp eggs). A small tank was used, which had a separator dividing the tank into two portions. The simulated seawater was poured into the tank followed by the addition of 1.5 g shrimp eggs/L in one portion of the tank, which was then covered with aluminium foil. Brine shrimp eggs were allowed to hatch for 48 hours until mature nauplii (larvae) were obtained. During hatching, oxygen supply was maintained. By utilizing a perforated dam, the mature nauplii moved towards a lamp light placed at the other portion of the tank. This bioassay utilized these mature nauplii [45].

Test samples (1000 µg/mL, 500 µg/mL, 100 µg/mL, 50 µg/mL, 10 µg/mL and 5 µg/mL) were made in seawater (artificial). 5% DMSO was used for dissolving the compounds which were water-insoluble, and then seawater was added. DMSO and doxorubicin were maintained to obtain negative control and positive control values, respectively. In 96-well microplates each sample was added in triplicate. Ten larvae of the brine shrimp were transferred to each well of the 96-well microplates containing different test sample concentrations. The microwell plate was then covered and incubated for 24 hours at 22-29 ºC. By using a microscope/magnifying glass, the nauplii which were dead (non-mobile) were counted in all the wells, and after recording the percent mortality, LC_{50} values were calculated by using GraphPad Prism (GraphPad Prism software Version 6.01) software [39, 46].

5.4.2. Potato Disc Tumour Induction Assay

Agrobacterium tumefaciens (A.tumefaciens), a tumour-inducing gram-negative bacteria, was incubated at 28ºC for two days (48 hrs) using yeast extract media (YEM) which was autoclaved at 121ºC for 15 minutes. Disease-free (fresh) potato tubers were cleaned with a brush under tap water, then soaked for 20 minutes in 10% bleach. After removing the potatoes from the bleach, the skins were removed and then they were sterilized again by immersing in liquid bleach for 10 minutes. With a sterilized cork borer, a core cylinder was removed from each potato. Under aseptic conditions, uniform discs of 0.5 cm were cut from the cylinder and transferred to the already prepared petri dishes containing 1.5% agar (1.5 gm agar/100 mL distilled water, about 25 mL was poured in each sterilized petri dish). Five potato discs were placed inside each petri plate. The whole process from potato cutting to inoculations was conducted in approximately 30 minutes (to avoid contamination) [39, 47].

The inoculum was made by mixing 400 µL of each concentration (1000 µg/mL, 500 µg/mL, 100 µg/mL, 50 µg/mL, 10 µg/mL and 5 µg/mL) with 400µL of A.tumefaciens bacterium suspension and then 50µL of each inoculum was separately applied over the surface of individual potato discs. All petri dishes were incubated for twenty-one days at 28ºC. After incubation, Lugol's solution (5% I_2 and 10% KI) was used for staining (15 minutes). The potato starch was stained dark blue/brown by Lugol's reagent whereas the tumours were not stained and appeared creamy to orange under a dissecting microscope. The total number of tumours were counted on each disc. Analyses were performed in triplicate. Tumour percentage inhibition was determined by using the formula:

$$\text{Percentage inhibition} 1 - \frac{\text{Average No. of tumours in sample}}{\text{Average No. of tumours in} - \text{ve control}} \times 100$$

Finally, IC_{50} values were calculated for individual compounds using GraphPad Prism software Version 6.01 [48].

RESULTS AND DISCUSSION

1. Infra-Red (IR) Spectral Analysis of Ligands and Metal Complexes

All the ligands and their respective iron(III) and zinc(II) metal complexes were identified using FTIR spectra. Table 1 represents spectral data (IR) of all the ligands and their metal complexes. The stretching vibrations C≡N, C=O, C=C, N-H, C-O and N-M (nitrogen-metal) were obtained for structural confirmation of the ligands and metal complexes. Desired compounds and proposed structures were found in agreement, as indicated by the stretching vibration data of functional groups in Table 1. The IR spectrum of $(L3)_2Zn$ is illustrated in Figure 10.

The N-H bands for ligands 2 and 3 appeared at 3444 cm^{-1} and 3395 cm^{-1}, but no NH band appeared in the spectra of metal complexes, which strongly supports the theory that a metal complex is formed through an N-M bond by replacing the hydrogen attached with the nitrogen. The band for C≡N was observed at 2250 cm^{-1}, 2265 cm^{-1} and 2340 cm^{-1} for Ligand 1 and its

iron(III) and zinc(II) metal complexes, respectively. The band for C=O was observed at 1642 cm^{-1} (Ligand 1), 1720 cm^{-1} (ligand 2) and 1747cm^{-1} (ligand 3) and their respective iron(III) (1738 cm^{-1}, 1717 cm^{-1}, 1739 cm^{-1}) and zinc(II) (1698 cm^{-1}, 1705 cm^{-1}, 1710 cm^{-1}) metal complexes. Whereas, the C-O band was observed at 1209 cm^{-1} (Ligand 1), 1263 cm^{-1} (Ligand 2) and 1132 cm^{-1} (Ligand 3) and their respective iron(III) (1024 cm^{-1}, 1120 cm^{-1}, 1295 cm^{-1}) and zinc(II) (1007 cm^{-1}, 1022 cm^{-1}, 1069 cm^{-1}) metal complexes. The N-M band was absent in L1, L2 and L3, whereas the appearance of the N-M band at 513 cm^{-1}, 487 cm^{-1}, 483 cm^{-1}, 543 cm^{-1}, 449 cm^{-1} and 469 cm^{-1} for iron(III) and zinc(II) metal complexes of ligand L1, L2 and L3 respectively, strengthens the theory of metal complex formation.

Table 1. IR data of Ligands and metal complexes

Compounds	C≡N (cm^{-1})	C=O (cm^{-1})	C=C (cm^{-1})	N-H (cm^{-1})	C-O (cm^{-1})	N-M (cm^{-1})
Ligand 1	2250	1642	1514	-	1209	-
$L1FeCl_3$	2265	1738	1475	-	1024	513
$L1Zn(Ac)_2$	2340	1698	1503	-	1007	478
Ligand 2	-	1720	1590	3444	1263	-
$(L2)_2FeCl$	-	1717	1521	-	1120	483
$(L2)_2Zn$	-	1705	1593	-	1022	543
Ligand 3	-	1747	1596	3395	1132	-
$(L3)_2FeCl$	-	1739	1532	-	1295	449
$(L3)_2Zn$	-	1710	1551	-	1069	469

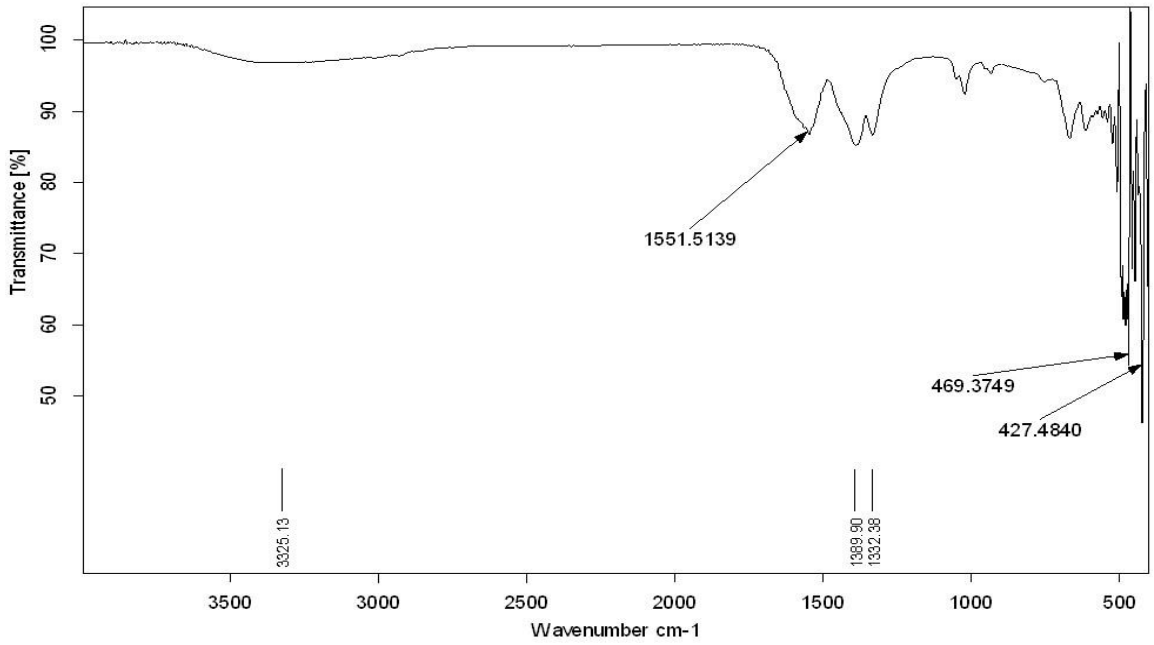

Figure 10. IR Spectrum of $(L3)_2Zn$

2. NMR Analysis

2.1. ^{1}H NMR Analysis

^{1}H NMR data of Ligand 1, L1$FeCl_3$, L1$Zn(Ac)_2$, Ligand 2, $(L2)_2$FeCl, $(L2)_2$Zn, Ligand 3, $(L3)_2$FeCl and $(L3)_2$Zn are reported in Table 2.

Distinct multiplicity and resonance intensity patterns are the features to focus on when assigning the signals to be integrated from ^{1}H NMR spectra. The ^{1}H NMR spectra of Ligand 2 and Ligand 3 showed that the proton signal bonded to the free ligand's nitrogen (δ = 3.10 ppm and δ = 3.12 ppm) was absent in the ^{1}H NMR spectra of the iron(III) and zinc(II) metal complexes of Ligand 2 and Ligand 3. The proton signals for the methoxy group of all the ligands and metal complexes appeared in the range of δ = 3.30-3.91 ppm. The proton signals for the phenyl substituent of Ligand 1 and its metal complexes were observed between δ = 7.50 and 7.65 ppm. The ^{1}H NMR spectra of Ligand 1 and $(L3)_2$Zn are presented in Figures 11 and 12, respectively.

2.2. ^{13}C NMR analysis

The ^{13}C NMR data of Ligand 1, L1$FeCl_3$, L1$Zn(Ac)_2$, Ligand 2, $(L2)_2$FeCl, $(L2)_2$Zn, Ligand 3, $(L3)_2$FeCl and $(L3)_2$Zn are reported in Table 3. The proposed structures of all the ligands and their respective iron(III) and zinc(II) metal complexes are strongly supported by the chemical shift values that appear in the ^{13}C NMR spectra. The free ligand's coordination with the metal atoms led to an upfield shift in the ^{13}C NMR spectra. The appearance of peaks for the additional two carbons in the range of δ = 160.3-177.9 ppm, confirmed the proposed structures of zinc(II) complex of Ligand 1. The CH_3 peaks for all the compounds appeared between δ = 55.1-67.5 ppm. The phenyl signals for Ligand 1 and its metal complexes appeared at δ = 28.6 ppm and 128.7 ppm. ^{13}C NMR spectra of Ligand 1 and $(L3)_2$Zn are presented in Figures 13 and 14, respectively.

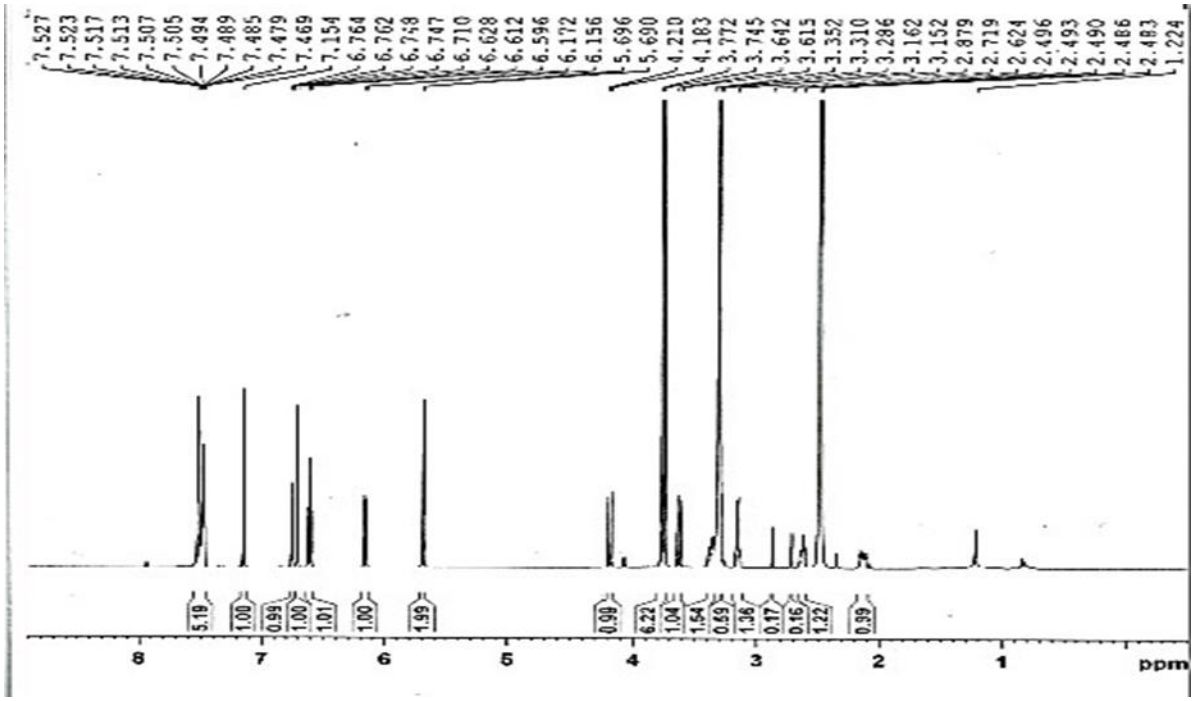

Figure 11. ^{1}H NMR Spectrum of Ligand 1

Table 2. ^{1}H NMR data of Ligands and their respective iron(III) and zinc(II) metal complexes.

H.no	Ligand 1		$L1FeCl_3$		$L1Zn(Ac)_2$		Ligand 2		$(L2)_2FeCl$		$(L2)_2Zn$		Ligand 3		$(L3)_2FeCl$		$(L3)_2Zn$	
	R	δ (ppm)	R	δ (ppm)	R	δ (ppm)	R	δ (ppm)	R	δ (ppm)	R	δ (ppm)	R	δ (ppm)	R	δ (ppm)	R	δ (ppm)
1	---	---	---	---	---	---	---	---	---	---	---		---	---	---	---	---	---
2	---	---	---	---	---	---	---	---	---	---	---	---	---	---	---	---	---	---
3	CH_2	6.50	CH_2	6.51	CH_2	6.53	CH_2	6.70	CH_2	6.73	CH_2	6.72	CH_2	6.73	CH_2	6.75	CH_2	6.72
4	CH_2	6.60	CH_2	6.63	CH_2	6.63	CH_2	6.72	CH_2	6.70	CH_2	6.71	CH_2	6.72	CH_2	6.70	CH_2	6.69
5	CH	6.73	CH	6.73	CH	6.73	CH	7.51	CH	7.53	CH	7.54	CH	7.54	CH	7.52	CH	7.51
6	---	---	---	---	---	---	---	---	---	---	---	---	---	---	---	---	---	---
7	---	---	---	---	---	---	---	---	---	---	---	---	---	---	---	---	---	---
8	CH	6.70	CH	6.70	CH	6.70	CH	6.63	CH	6.63	CH	6.64	CH	7.50	CH	7.51	CH	7.50
11	CH_3	3.31	CH_3	3.31	CH_3	3.31	CH_3	3.34	CH_3	3.34	CH_3	3.34	CH_3	3.36	CH_3	3.35	CH_3	3.36
11'	CH_3	3.32	CH_3	3.32	CH_3	3.32	CH_3	3.34	CH_3	3.35	CH_3	3.34	CH_3	3.35	CH_3	3.36	CH_3	3.36
12	---	---	---	---	---	---	---	---	---	---	---	---	---	---	---	---	---	---
13	CH	6.74	CH	6.71	CH	6.77	CH	7.53	CH	7.55	CH	7.54	---	---	---	---	---	---
15	---	---	---	---	---	---	---	---	---	---	---	---	CH	6.94	CH	6.95	CH	6.93
16	CH	6.76	CH	6.81	CH	6.83	CH	6.93	CH	6.95	CH	6.97	CH	6.67	CH	6.67	CH	6.67
17	CH	6.77	CH	6.82	CH	6.85	CH	6.91	CH	6.93	CH	6.95	CH	6.93	CH	6.93	CH	6.92
18	CH_2	6.63	CH_2	6.67	CH_2	6.65	CH_2	2.60	CH_2	2.67	CH_2	2.63	CH_2	2.66	CH_2	2.65	CH_2	2.63
19	CH_2	7.15	CH_2	7.17	CH_2	7.19	CH_2	3.70	CH_2	3.73	CH_2	3.71	CH_2	3.71	CH_2	3.73	CH_2	3.70
20	C_6H_6	7.50	C_6H_6	7.60	---	---	COOH	11.50	COOH	11.20	COOH	11.40	COOH	11.40	COOH	11.30	COOH	11.21
21					---	---	---	---	---	---	---	---	---	---	---	---	---	---
22					CH_3	3.30	---	---	---	---	---	---	---	---	---	---	---	---
					C_6H_6	7.65	NH	3.12	---	---	---	---	NH	3.10	---	---	---	---

Table 3. ^{13}C NMR data of Ligands and their respective iron(III) and zinc(II) metal complexes.

H.no	Ligand 1		$L1FeCl_3$		$L1Zn(Ac)_2$		Ligand 2		$(L2)_2FeCl$		$(L2)_2Zn$		Ligand 3		$(L3)_2FeCl$		$(L3)_2Zn$	
	R	δ (ppm)	R	δ (ppm)	R	δ (ppm)	R	δ (ppm)	R	δ (ppm)	R	δ (ppm)	R	δ (ppm)	R	δ (ppm)	R	δ (ppm)
1	C	124.1	C	125.0	C	125.5	C	146.6	C	146.7	C	146.8	C	147.9	C	147.8	C	147.7
3	CH_2	37.0	CH_2	37.5	CH_2	37.6	CH_2	39.2	CH_2	39.4	CH_2	39.3	CH_2	38.7	CH_2	38.6	CH_2	38.5
4	CH_2	27.1	CH_2	27.3	CH_2	27.4	CH_2	38.4	CH_2	38.6	CH_2	38.7	CH_2	37.1	CH_2	37.0	CH_2	36.9
5	CH	115.3	CH	115.3	CH	115.3	CH	111.1	CH	111.1	CH	111.1	CH	111.3	CH	111.3	CH	111.3
6	C	146.7	C	146.7	C	146.7	C	178.2	C	178.2	C	178.2	C	146.9	C	146.9	C	146.9
7	C	146.5	C	146.5	C	146.5	C	177.2	C	177.3	C	177.2	C	147.9	C	147.8	C	147.7
8	CH	113.4	CH	113.4	CH	113.4	CH	110.8	CH	110.9	CH	110.8	CH	111.4	CH	111.2	CH	111.0
9	C	136.4	C	136.7	C	136.9	C	167.7	C	167.8	C	167.9	C	127.3	C	127.0	C	126.8
10	C	136.4	C	136.6	C	136.8	C	173.6	C	173.7	C	173.8	C	126.5	C	126.3	C	126.1
11	CH_3	55.5	CH_3	55.5	CH_3	55.5	CH_3	55.2	CH_3	55.2	CH_3	55.2	CH_3	55.5	CH_3	55.5	CH_3	55.5
11'	CH_3	55.8	CH_3	55.8	CH_3	55.8	CH_3	55.1	CH_3	55.1	CH_3	55.1	CH_3	55.4	CH_3	55.4	CH_3	55.4
12	C	136.4	C	137.0	C	137.3	C	100.3	C	100.6	C	100.7	C	124.5	C	124.0	C	124.3
13	CH	113.4	CH	113.5	CH	113.7	CH	124.0	CH	124.0	CH	124.0	C	146.8	C	146.7	C	146.6
14	C	148.8	C	148.7	C	148.9	C	124.3	C	124.3	C	124.3	C	146.6	C	146.6	C	146.6
15	C	147.2	C	147.3	C	147.4	C	124.3	C	124.4	C	124.5	CH	104.3	CH	104.3	CH	104.3
16	CH	115.3	CH	115.5	CH	115.5	CH	114.0	CH	114.0	CH	114.0	CH	121.0	CH	121.0	CH	121.0
17	CH	120.0	CH	121.0	CH	121.5	CH	120.7	CH	121.5	CH	121.6	CH	107.1	CH	107.0	CH	106.9
18	CH_2	45.0	CH_2	47.0	CH_2	47.7	CH_2	36.7	CH_2	37.0	CH_2	37.3	CH_2	25.6	CH_2	25.7	CH_2	25.5
19	CH_2	101.5	CH_2	101.6	CH_2	101.7	CH_2	51.5	CH_2	51.7	CH_2	51.6	CH_2	100.9	CH_2	100.6	CH_2	100.3
20	C	170.0	C	170.9	C	171.7	COOH	181.1	COOH	182.0	COOH	183.0	COOH	180.3	COOH	179.7	COOH	179.3
21	CN	127.0	CN	127.2	CN	127.3	---	---	---	---	---	---	---	---	---	---	---	---
22	C_6H_6	128.6	C_6H_6	128.7	CH_3	160.3	---	---	---	---	---	---	---	---	---	---	---	---
23					C	173.7	---	---	---	---	---	---	---	---	---	---	---	---

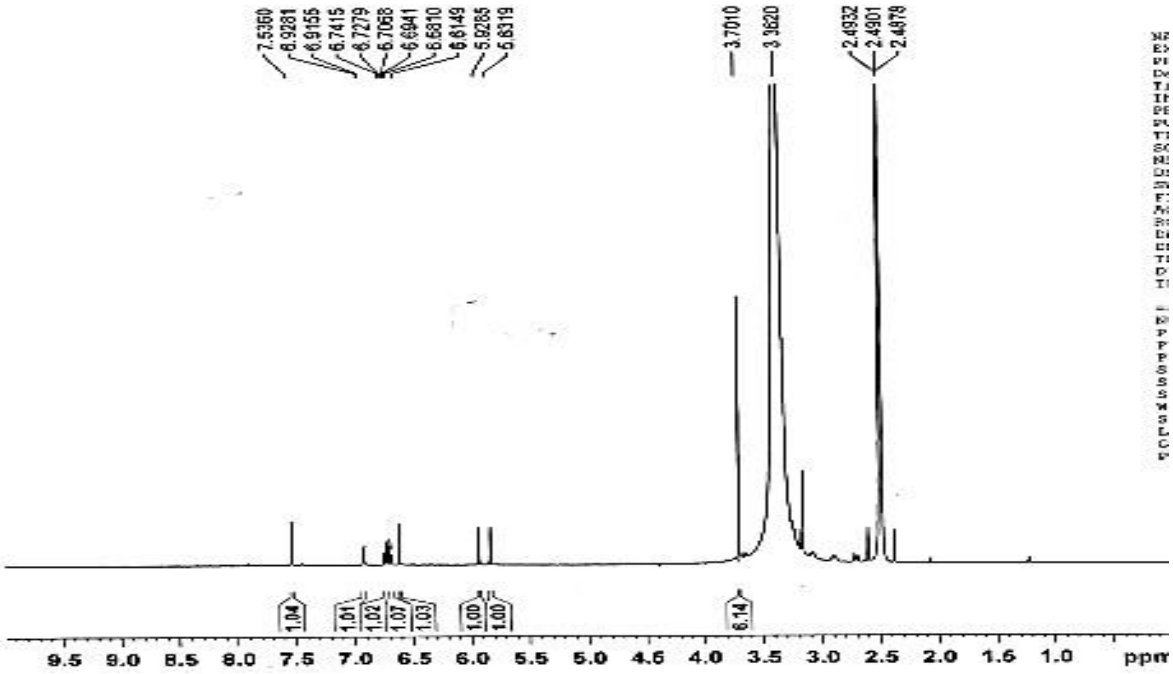

Figure 12. ^{1}H NMR Spectrum of $(L3)_2Zn$

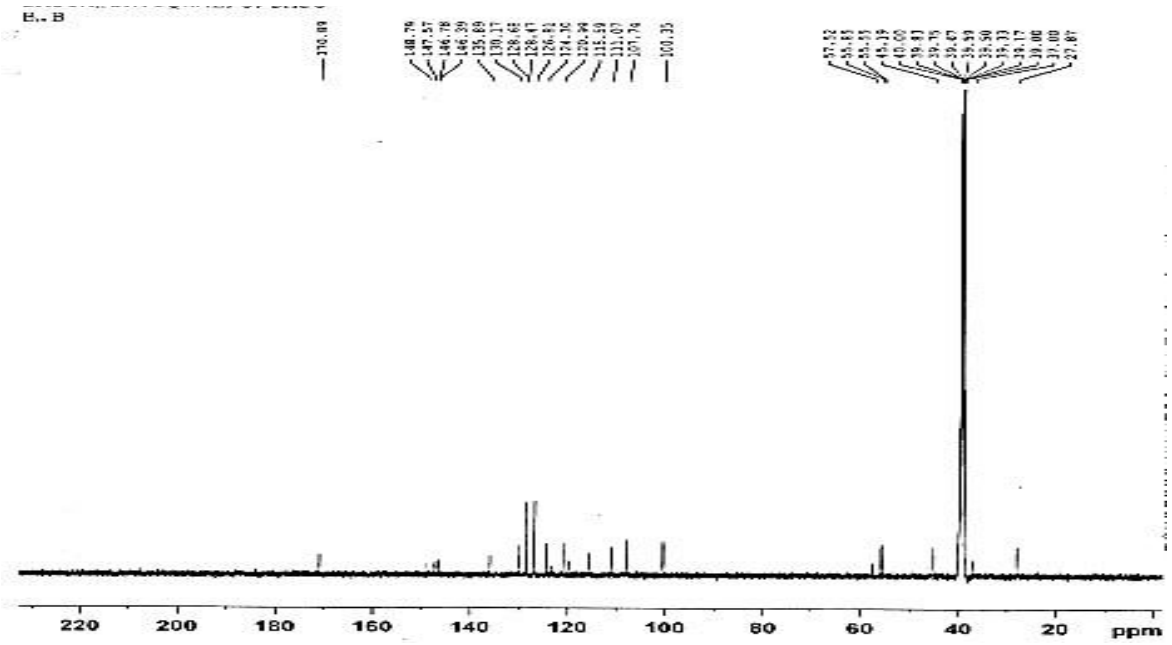

Figure 13. ^{13}C NMR Spectrum of Ligand 1

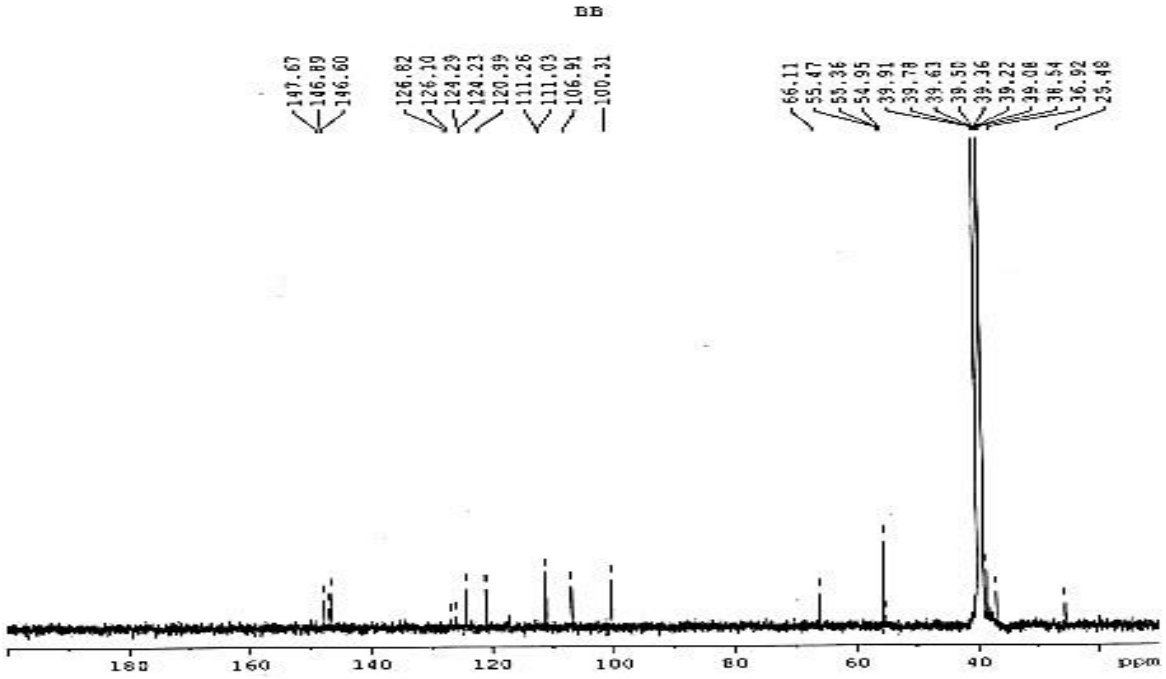

Figure 14. ^{13}C NMR Spectrum of $(L3)_2Zn$

Table 4. Mass spectral analysis data of Ligand 1, 2 and 3.

Ligand 1		Ligand 2		Ligand 3	
Mass	% base	Mass	% base	Mass	% base
429.2	17.3	326.1	57.8	326.1	54.2
400.2	6.5	310.1	7.5	310.1	7.2
370.2	6.6	294.0	49.9	294.1	25.1
321.2	89.7	280.0	4.9	280.1	3.9
294.1	4.4	236.1	100.0	252.1	3.1
216.1	1.6	190.0	43.6	236.0	100.0
135.0	4.8	175.0	7.4	192.0	36.8
104.9	100.0	135.0	6.1	175.0	5.1
77.0	34.8	105.0	5.3	146.0	2.8
50.9	6.5	77.0	8.3	134.9	4.5
---	---	43.9	8.5	105.0	2.9
---	---	---	---	77.0	7.4
---	---	---	---	50.9	4.4

3. Mass Spectral Analysis

High-resolution mass spectrometry was used for the acquisition of mass spectra. The mass spectral analysis data of the Ligands 1, 2 and 3 are represented in Table 4.

Mass spectra of all ligands were acquired with a high-resolution mass spectrometer. The molecular ion peaks were recorded at 429.2 m/z for Ligand 1and 326.1 m/z for Ligand 2 and Ligand 3. The molecular ion peaks of Ligand 2 and Ligand 3 are similar. The values of base peaks were noted at 104.9 for Ligand 1, 236.1 for Ligand 2 and 236.0 for Ligand 3. All the data for the molecular ion peaks, base peaks and other peaks are in accordance with the fragmentation pattern of the ligands. The mass spectrum of Ligand 1 is shown in Figure 15. It was not possible to get mass spectral data for the iron(III) and zinc(II) metal complexes due to the lower stability of the prepared complexes.

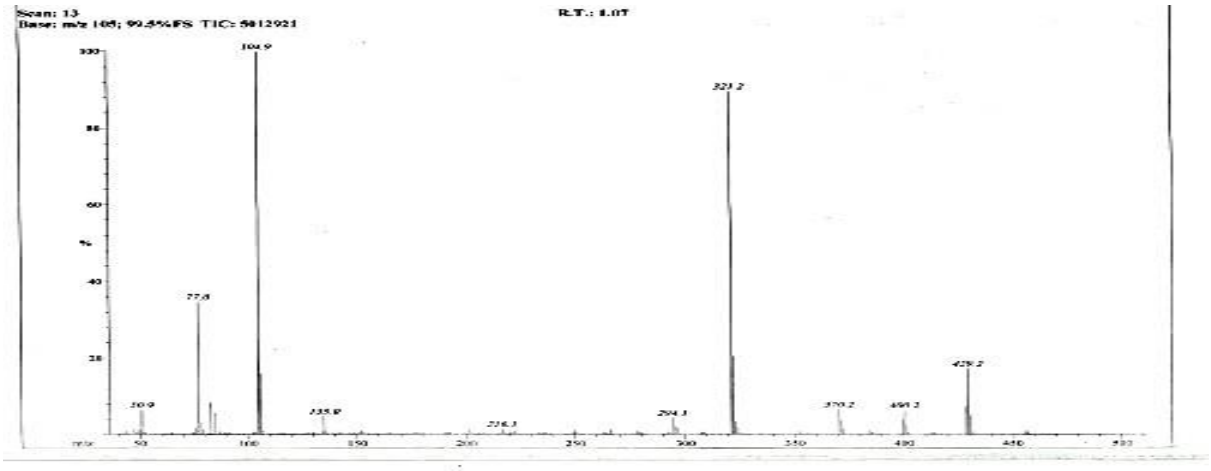

Figure 15. Mass spectrum of Ligand 1

Table 5. Antibacterial activity of Ligands and their metal complexes

Compound	Zone of inhibition (mm)		
	Escherichia coli	*Pseudomonas aeruginosa*	*Staphylococcus aureus*
Ligand 1	12	13	14
$L1FeCl_3$	18	18	14
Ligand 2	13	16	13
$(L2)_2FeCl$	14	17	14
$(L2)_2Zn$	16	19	23
Ligand 3	15	14	13
$(L3)_2FeCl$	16	15	15
$(L3)_2Zn$	17	20	20
Reference drug (Tetracycline)	25	20	23

4. Bioassays

4.1. Antibacterial Activity

The agar well diffusion method was used for antibacterial evaluation of all the ligands and metal complexes against *Escherichia coli* and *Staphylococcus aureus* (gram-negative strains) and *Pseudomonas aeruginosa* (gram-positive strain). The results of antibacterial screening (conducted in-vitro) in terms of zone of inhibition observed in millimetre (mm), are given in Table 5.

The reference drug used was tetracycline. All the ligands showed some activity against each bacterial species, but the metal complexes showed better activities in comparison to the original ligands, and all zinc(II) complexes proved to be good antibacterial agents. The zinc(II) complex of Ligand 1 showed promising activity against the *Staphylococcus aureus* strain.

4.2. Antifungal Activity

Antifungal screening of all the ligands and metal complexes was conducted by employing well-in-agar method against two *Candida* species (*Candida albicans* and *Candida glabrata*). After a 48 hour incubation period at 28ºC, inhibition zones around the wells were observed and recorded in millimetres (mm). The antifungal activity results are summarised in Table 6.

Nystatin was used as a standard drug. All the compounds expressed better antifungal activity against *Candida albicans* compared to Candida glabrata. Metal complexes illustrated better antifungal activities compared to the free ligands, especially zinc(II) complexes. The zinc(II) complex of Ligand 3 showed exceptional activity against the *Candida albicans* strain.

Table 6. Antifungal activity of Ligands and metal complexes

Compound	Zone of inhibition (mm)	
	Candida albican	*Candida glabrata*
Ligand 1	11	10
$L1FeCl_3$	11	10.2
$L1Zn(Ac)_2$	19	10.2
Ligand 2	10	<10
$(L2)_2FeCl$	14	10.8
$(L2)_2Zn$	20	10.5
Ligand 3	11	<10
$(L3)_2FeCl$	15	14
$(L3)_2Zn$	21	12
Reference drug (nystatin)	19	16

Table 7. Antioxidant activity (DPPH free radical scavenging activity of Ligands and metal complexes with IC_{50} values)

Compound	% Scavenging effect at different concentrations (µg/mL)						IC_{50} (µg/mL)
	1000	500	100	50	10	5	
Ligand 1	95.1±0.64	92.9±0.56	92.5±0.72	91.5±0.61	91.1±0.64	90.8±0.63	0.98
$L1FeCl_3$	88.0±0.47	87.8±0.51	87.7±0.32	87.4±0.77	86.8±0.76	85.7±0.67	1.31
$L1Zn(Ac)_2$	90.9±0.33	90.6±0.55	89.3±0.22	89.9±0.66	87.2±0.33	86.9±0.72	1.23
Ligand 2	84.3±0.57	90.4±0.21	88.9±0.37	88.6±0.49	88.5±0.83	87.8±0.54	1.17
$(L2)_2FeCl$	72.6±0.33	84.7±0.41	83.8±0.90	82.9±0.53	82.2±0.72	81.8±0.44	1.74
$(L2)_2Zn$	75.5±0.44	88.4±0.22	87.9±0.88	87.6±0.35	86.6±0.67	85.5±0.59	1.33
Ligand 3	89.9±0.33	89.6±0.49	88.4±0.57	88.3±0.23	87.8±0.31	87.0±0.67	1.22
$(L3)_2FeCl$	87.6±0.57	87.3±0.53	87.2±0.65	86.2±0.39	85.9±0.84	85.4±0.29	1.37
$(L3)_2Zn$	90.3±0.47	89.2±0.66	88.5±0.81	88.4±0.69	87.9±0.53	87.4±0.84	1.25
Ascorbic acid	92.4±0.56	90.2±0.58	89.9±0.58	89.5±0.57	88.8±0.58	88.2±0.64	1.14

4.3. Antioxidant Activity

A DPPH assay was used for antioxidant activity evaluation. The percentage scavenging effect at various concentrations was calculated, and a standard error mean (SEM) was determined, e.g. Ligand 1 at 1000 µg/mL has % scavenging effect 89.1 ± 0.54 %. Finally, GraphPad Prism Software Version 6.01 calculated IC_{50} values. The results are compiled in Table 7. The smaller the IC_{50} value, the greater the antioxidant activity.

Amongst all, Ligand 1 showed promising antioxidant activity. As the experiment was conducted in triplicate, standard error mean (SEM) and IC_{50} values were calculated using GraphPad Prism Software Version 6.01.

4.4. Cytotoxicity Assays

4.4.1. Brine-Shrimp Microwell Cytotoxicity Assay

Leach, i.e. Artemia salina (brine shrimp eggs) was used in this cytotoxicity assay. Ten larvae of the brine shrimps were transferred to each well along with the test samples and the seawater. After 24 hours, the total number of shrimps killed at different concentrations were recorded, and as the experiment was conducted in triplicate, a standard error mean (SEM) was calculated. Finally, LC_{50} values were calculated by using GraphPad Prism Software Version 6.01. The results of brine shrimp microwell cytotoxicity assay are stated in Table 8. The smaller the LC_{50} value of the compound, the greater will be the antitumor activity possessed by the compound.

Table 8. Brine shrimp microwell cytotoxicity assay result.

Compound	Total shrimps killed at different concentrations (µg/mL)						LC_{50}
	1000	500	100	50	10	5	(µg/mL)
Ligand 1	3.0±0.7	2.6±0.9	2.0±1.6	1.6±0.7	1.3±0.9	1.0±1.3	1668.00
$L1FeCl_3$	3.0±0.8	2.0±0.6	1.6±0.8	1.3±0.8	1.0±0.8	1.0±1.6	1977.00
$L1Zn(Ac)_2$	4.0±0.5	3.3±0.7	2.3±0.6	2.0±0.6	1.6±0.8	1.0±1.1	1055.00
Ligand 2	6.0±0.6	4.6±0.7	4.0±0.4	2.0±0.8	1.6±1.1	1.0±1.6	408.40
$(L2)_2FeCl$	6.6±0.7	5.3±0.6	4.3±0.7	2.3±0.5	1.6±1.4	1.0±0.5	275.00
$(L2)_2Zn$	7.0±0.8	6.0±0.7	4.6±0.8	2.6±0.8	1.6±1.5	1.0±0.9	194.50
Ligand 3	3.3±0.4	3.0±0.5	2.6±0.8	2.3±0.7	1.3±1.3	1.0±0.9	1310.00
$(L3)_2FeCl$	3.0±0.9	3.0±1.4	2.3±0.5	2.0±0.8	1.0±1.3	1.0±1.7	1477.00
$(L3)_2Zn$	4.0±0.7	3.6±0.6	3.0±0.4	2.6±0.9	1.6±1.5	1.0±1.3	904..30
Doxorubicin	10.0±0.0	10.0±0.0	10.0±0.0	8.0±0.0	7.0±0.6	5.0±0.9	5.79

Table 9. Potato disc tumour induction assay results

Compound	Percentage inhibition of tumour growth at different concentrations (µg/mL)						IC_{50} (µg/mL)
	500	100	50	10	5		
Ligand 1	70.83	54.16	52.08	50.00	47.92	45.83	50.55
$L1FeCl_3$	65.33	50.50	48.90	46.33	42.67	39.90	94.62
$L1Zn(Ac)_2$	70.00	53.50	52.00	49.90	47.50	45.33	53.03
Ligand 2	95.83	91.67	87.50	75.00	70.83	66.67	4.66
$(L2)_2FeCl$	80.33	76.67	70.90	66.67	61.33	55.50	7.96
$(L2)_2Zn$	90.90	85.50	81.33	72.50	66.90	61.67	5.66
Ligand 3	91.63	89.58	87.50	79.16	77.08	75.00	3.65
$(L3)_2FeCl$	81.67	76.00	70.67	68.90	64.50	58.00	6.93
$(L3)_2Zn$	85.00	80.90	78.67	70.00	66.90	62.67	5.75

Negative control = 5% DMSO = 24 tumors/disc
Positive control = 250 µg/ml vincristine = 2 tumors /disc = 91.67 % tumor inhibition

4.4.2. Potato Disc Tumor Induction Assay

Another toxicity assay performed was the potato disc tumour induction assay. The tumour was induced in potato discs utilizing the Agrobacterium tumefaciens strain. The antitumour effect of all the compounds was determined by applying each compound over the surface of individual potato discs. After incubation, tumour percentage inhibition for different concentrations of all the compounds was determined, and IC_{50} values for individual compounds were calculated using GraphPad Prism Software Version 6.01. The results of the potato disc tumour induction assay are reported in Table 9. The smaller the IC_{50} value of the compound, the greater the antitumour characteristics of the compound. All the compounds showed some antitumour effect against Agrobacterium tumefaciens strains. The free ligands proved themselves to be better antitumour agents. The antitumour activity shown by Ligand 3 and $(L3)_2Zn$ is worth mentioning, and further research to explore the mechanism of action of such moieties is anticipated.

CONCLUSION

This research focused on tetrahydrobenzylisoquinoline alkaloid derivatives (Ligand1, Ligand 2 and Ligand 3), which were used as free ligands. Their iron(III) and zinc(II) metal complexes were synthesized, followed by physical and spectral characterization and then these were screened through bioassays including antibacterial, antifungal, antioxidant and cytotoxicity assays (brine-shrimp microwell cytotoxicity assay and potato disc tumour induction assay). All the physical and spectral characterization data supported the proposed structures of all the ligands and their respective iron(III) and zinc(II) metal complexes.

All the ligands showed antimicrobial activity, but

the metal complexes indicated better antimicrobial activity than the original ligands, especially all zinc(II) complexes. All the compounds presented better antifungal activity against *Candida albicans* compared to *Candida glabrata*. The free ligands (especially Ligand 1) revealed better antioxidant behaviour compared to the metal complexes. All the compounds exposed some toxic behaviour for brine shrimp eggs and antitumour behaviour against the Agrobacterium tumefaciens strain, proving that the compounds have the potential to act as antitumour agents.

Overall, the compounds were pharmacologically active. Thus, further investigation to determine the mode of action of tetrahydrobenzylisoquinoline alkaloid derivatives and their metal complex formation is recommended.

ACKNOWLEDGEMENTS

The authors are thankful to the Universiti Malaya, Kuala Lumpur, Malaysia and Riphah International University, Islamabad, Pakistan, for providing research facilities to carry out the work.

DECLARATION OF INTERESTS

The authors declare that they have no known competing financial interests or personal relationships that could have appeared to influence the work reported in this paper.

REFERENCES

1. Finar, I. L., Organic Chemistry: Stereochemistry and the Chemistry of Natural Products. Volume Two. 1956: Longmans, Green and Company.

2. Dewick, P. M., Medicinal natural products: a biosynthetic approach. 2002: John Wiley & Sons.

3. Majumdar, K. C. and S. K. Chattopadhyay, Heterocycles in natural product synthesis. 2011: John Wiley & Sons.

4. Kawthekar, R. B., Peters, B. K., Govender, T., Kruger, H. G. and Maguire, G. E. (2015) Synthesis of (S)-3-aminoethyl-1, 2, 3, 4-tetrahydroisoquinoline (TIQ-diamine) via the Mitsunobu protocol. *South African Journal of Chemistry*, **63**, 195–198.

5. Dang, T. T. T., Onoyovwi, A., Farrow, S. C. and Facchini, P. J. (2012) 11 Biochemical Genomics for Gene Discovery in Benzylisoquinoline Alkaloid Biosynthesis in Opium Poppy and Related Species. *Methods in enzymology*, **515**, 231.

6. Talapatra, S. K. and Talapatra, B. (2015) Papaverine (l-Tyrosine-Derived Alkaloid), in Chemistry of Plant Natural Products. *Springer*, 803–809.

7. Cahlíková, L., Valterová, I., Macáková, K. and Opletal, L. (2011) Analysis of Amaryllidaceae alkaloids from Zephyranthes grandiflora by GC/MS and their cholinesterase activity. *Revista Brasileira de Farmacognosia*, **21(4)**, 575–580.

8. Guo, N., Yu, L., Meng, R., Fan, J., Wang, D., Sun, G. and Deng, X. (2008) Global gene expression profile of Saccharomyces cerevisiae induced by dictamnine. *Yeast*, **25(9)**, 631–641.

9. Lamoral-Theys, D., et. al. (2009) Lycorine, the main phenanthridine Amaryllidaceae alkaloid, exhibits significant antitumor activity in cancer cells that display resistance to proapoptotic stimuli: an investigation of structure− activity relationship and mechanistic insight. *Journal of medicinal chemistry*, **52(20)**, 6244–6256.

10. Morales-Rubio, M., Treviño Neávez, J. F.and Viveros Valdez, E. (2010) Free Radical Scavenging Activities of Lophocereus schottii (Engelmann. *Internatıonal Journal of Natural and Engineering Sciences (IJNES)*, **4(1)**, 65–68.

11. Obiero, G. O., Lutta, K. P., Akeng'a, T. and Cornelius, W. W. (2009) Antifeedant Activities of the Erythrinaline Alkaloids from Erythrina latissima against Spodoptera littoralis (Lepidoptera noctuidae).

12. Paulo, M. D. Q., Barbosa-Filho, J., Lima, E. O.,. Maia, R. F., De Cassia, R., Barbosa, B. and Kaplan, M. A. C. (1992) Antimicrobial activity of benzylisoquinoline alkaloids from Annona salzmanii DC. *Journal of ethnopharmacology*, **36(1)**, 39–41.

13. Ruchirawat, S. and Namsa-Aid, A. (2001) An efficient synthesis of argemonine, a pavine alkaloid. *Tetrahedron Letters*, **42(7)**, 1359–1361.

14. Scazzocchio, F., Cometa, M., Tomassini, L. and Palmery, M. (2001) Antibacterial activity of Hydrastis canadensis extract and its major isolated alkaloids. *Planta medica*, **67(6)**, 561–564.

15. Schmeller, T., Latz-Brüning, B. and Wink, M. (1997) Biochemical activities of berberine, palmatine and sanguinarine mediating chemical defence against microorganisms and herbivores. *Phytochemistry*, **44(2)**, 257–266.

16. Szlavik, L., Gyuris, A.,. Minarovits, J., Forgo, P., Molnar, J. and Hohmann, J. (2004) Alkaloids from Leucojum vernum and antiretroviral activity of Amaryllidaceae alkaloids. *Planta medica*, **70(9)**, 871–873.

17. Meggers, E. (2007) Exploring biologically relevant chemical space with metal complexes. *Current opinion in chemical biology*, **11(3)**, 287–292.

18. Ismail, A. H., Al-Bairmani, H. K., Abbas, Z. S. and Rheima, A. M (2020) Nano metal-complexes of theophylline derivative: synthesis, characterization, molecular structure studies, and antibacterial activity. in IOP Conference Series: Materials Science and Engineering. *IOP Publishing*.

19. Gacki, M., Kafarska, K., Pietrzak, A., Korona-Głowniak, I. and Wolf, W. M. (2020) Double Palindrome Water Chain in Cu (II) Theophylline Complex. Synthesis, Characterization, Biological Activity of Cu (II), Zn (II) Complexes with Theophylline. *Crystals*, **10(2)**, 97.

20. Zaidi, M. I., Wattoo, F. H., Wattoo, M. H. S., Tirmizi, S. A. and Salman, S. (2012) Antibacterial activities of nicotine and its zinc complex. *African Journal of Microbiology Research*, **6(24)**, 5134-5137.

21. Knolker, H.-J. (2004) Transition metal complexes in organic synthesis, part 70#. Synthesis of biologically active carbazole alkaloids using organometallic chemistry. *Current Organic Synthesis*, **1(4)**, 309–331.

22. Patnaik, P. (2002) Handbook of Inorganic Chemical Compounds McGraw-Hill handbooks. *McGraw-Hill Professional*, **1086**.

23. Turova, N. Y., Turevskaya, E. P., Kessler, V. G. and Yanovskaya, M. I. (2006) The chemistry of metal alkoxides. *Springer Science & Business Media*.

24. Veith, M., Grätz, F. and Huch, V. (2001) Fe_9O_3 (OC_2H_5) 21 C_2H_5OH− A New Structure Type of an Uncharged Iron (III) Oxide− Alkoxide Cluster. *European Journal of Inorganic Chemistry*, **2001(2)**, 367–368.

25. Aas, H. (1971) The Silgrain Process, Silicon Metal from 90% Ferrosilicon.

26. Greenwood, N. and Earnshaw, A. (1997) Chemistry of the Elements 2nd Edition. Butterworth-Heinemann.

27. Seisenbaeva, G. A., Gohil, S., Suslova, E. V., Rogova, T. V., Turova, N. Y. and Kessler, V. G. (2005) The synthesis of iron (III) ethoxide revisited: Characterization of the metathesis products of iron (III) halides and sodium ethoxide. *Inorganica chimica acta*, **358(12)**, 3506–3512.

28. Furnell, B. (1989) Vogel'Text Book of Practical Organic Chemistry, Longman/Wiley, New York.

29. Sarwar, A., Saharin, S. M., Bahron, H. and Alias, Y. (2020) Synthesis, structures, luminescence and thermal stability of Visible/NIR emitting binuclear azomethine-Zn (II) complexes. *Journal of Luminescence*, **223**,117227.

30. Hemilä, H. (2011) Zinc lozenges may shorten the duration of colds: a systematic review. *The open respiratory medicine journal*, **5**, 51.

31. Williams, D. B. G. and Lawton, M. (2010) Drying of organic solvents: quantitative evaluation of the efficiency of several desiccants. *The Journal of organic chemistry*, **75(24)**, 8351–8354.

32. Furniss, B. S. (1989) Vogel's textbook of practical organic chemistry. *Pearson Education India*.

33. Naureen, B., Miana, G. A., Shahid, K., Asghar, M., Tanveer, S.and Sarwar, A. (2021) Iron (III) and zinc (II) monodentate Schiff base metal complexes: Synthesis, characterisation and biological activities. *Journal of Molecular Structure*, **129946**.

34. Batool, A., Shahid, K. and Muddasir, M. (2015) Synthesis of aniline derivative of ursolic acid, its metal complexes, characterization and bioassay, **30**, 25–32.

35. Kurahashi, T., Oda, K., Sugimoto, M., Ogura, T. and Fujii, H. (2006) Trigonal-bipyramidal geometry induced by an external water ligand in a sterically hindered iron salen complex, related to the active site of protocatechuate 3, 4-dioxygenase. *Inorganic chemistry*, **45(19)**, 7709–7721.

36. Mayilmurugan, R., Sankaralingam, M., Suresh, E.and Palaniandavar, M. (2010) Novel square pyramidal iron (III) complexes of linear tetradentate bis (phenolate) ligands as structural

and reactive models for intradiol-cleaving 3, 4-PCD enzymes: Quinone formation vs. intradiol cleavage. *Dalton Transactions*, **39(40)**, 9611–9625.

37. Dey, S. K., Bag, B., Dey, D. K., Gramlich, V., Li, Y. and Mitra, S. (2003) Synthesis and characterization of copper (II) and zinc (II) complexes containing 1-phenyl-3-methyl-4-benzoyl-5-pyrazolone. *Zeitschrift für Naturforschung B*, **58(10)**, 1009–1014.

38. Diez-Castellnou, M., Salassa, G., Mancin, F. and Scrimin, P. (2019) The Zn (II)-1, 4, 7-trimethyl-1, 4, 7-triazacyclononane complex: a monometallic catalyst active in two protonation states. *Frontiers in chemistry*, **7**, 469.

39. Demirci, F. and Baser, K. H. C. (2002) Bioassay Techniques for Drug Development By Atta-ur-Rahman, M. Iqbal Choudhary (HEJRIC, University of Karachi, Pakistan), William J. Thomsen (Areana Pharmaceuticals, San Diego, CA). Harwood Academic Publishers, Amsterdam, The Netherlands. 2001. xii+ 223 pp. 15.5× 23.5 cm. $79.00. ISBN 90-5823-051-1. *Journal of Natural Products*, **65(7)**, 1086–1087.

40. Kumar, V. P., Chauhan, N. S., Padh, H. and Rajani, M. (2006) Search for antibacterial and antifungal agents from selected Indian medicinal plants. *Journal of ethnopharmacology*, **107(2)**, 182–188.

41. Scorzoni, L., Benaducci, T., Almeida, A., Silva, D. H. S., Bolzani, V. D. S., Giannini, M. and Soares, M. J. (2007) Comparative study of disk diffusion and microdilution methods for evaluation of antifungal activity of natural compounds against medical yeasts Candida spp and Cryptococcus sp, Revista de Ciências Farmacêuticas Básica e Aplicada, 25–34.

42. Ramamoorthy, P. K. T., Lakshmanashetty, R. H., Devidas, S., Mudduraj, V. T. and Vinayaka, K. S. (2012) Antifungal and cytotoxic activity of Everniastrum cirrhatum (Fr.) Hale. *Chiang Mai. J. Sci.*, **39(1)**, 76–83.

43. Nikolova, M., Evstatieva, L. and Nguyen, T. D. (2011) Screening of plant extracts for antioxidant properties. *Botanica Serbica*, **35(1)**, 43–48.

44. Sancak, K.., Ünver, Y., Ünlüer, D., Düğdü, E., Kör, G., Celik, F. and Birinci, E. (2012) Synthesis, characterization, and antioxidant activities of new trisubstituted triazoles. *Turkish Journal of Chemistry*, **36(3)**, 457–466.

45. Morshed, M., Hossain, M. S., Islam, M., Ali, M., Ibrahim, M., Islam, M. and Islam, M. A. (2005) Toxicity of four synthetic plant hormones IAA, NAA, 2, 4-D and GA against Artemia salina (Leach). *International Journal of Agriculture and Biology*, **7(2)**, 240–242.

46. Khan, I., Ahmad, K., Khalil, A. T., Khan, J., Khan, Y. A., Saqib, M. S., Umar, M. N. and Ahmad, H. (2015) Evaluation of antileishmanial, antibacterial and brine shrimp cytotoxic potential of crude methanolic extract of Herb Ocimum basilicum (Lamiacea). *Journal of Traditional Chinese Medicine*, **35(3)**, 316–322.

47. Coker, P., Radecke, J., Guy, C. and Camper, N. (2003) Potato disc tumor induction assay: a multiple mode of drug action assay. *Phytomedicine*, **10(2)**, 133–138.

48. Bhatti, M. Z., Ali, A., Saeed, A., Saeed, A. and Malik, S. A. (2015) Antimicrobial, antitumor and brine shrimp lethality assay of Ranunculus arvensis L. extracts. *Pak. J. Pharm. Sci*., **28(3)**, 945–949.